David Tomás Sánchez Martínez
Lourdes García Rodríguez
(coordinadores)

Proceedings of the 7th International Seminar on ORC Power Systems

Editorial Universidad de Sevilla

Proceedings of the 7th International Seminar on

ORC
Power Systems

David Tomás Sánchez Martínez
Lourdes García Rodríguez
(coordinadores)

Proceedings of the 7th International Seminar on

ORC Power Systems

(ORC2023)

4th to 6th
SEPTEMBER
SEVILLE 2023

EDITORIAL UNIVERSIDAD DE SEVILLA

Sevilla, 2024

Colección Actas
Núm.: 91

Review chairs of the 7th International Seminar on ORC Power Systems

Prof. Christoph Wieland (University of Duisburg-Essen) - *Review Chair*
Prof. Sotirios Karellas (National Technical University of Athens) - *Review Co-Chair*
Prof. Teemu Turunen-Saaresti (LUT University) - *Review Co-Chair*
Dr. Diego-César Alarcón-Padilla (Plataforma Solar de Almería - CIEMAT) - *Review Co-Chair*
Dr. Francesco Crespi (Universidad de Sevilla) - *Review Co-Chair*

ISBN 978-84-472-2745-7
DOI: https://dx.doi.org/10.12795/9788447227457

Diseño de cubierta y maquetación: los autores

INDEX OF CONTRIBUTIONS

DOI: https://dx.doi.org/10.12795/9788447227457_118

TES4TRIG: DEVELOPMENT OF A DEMONSTRATOR FOR THE PRODUCTION OF ELECTRICITY, HEATING AND COOLING BASED ON AN ORGANIC RANKINE CYCLE AND AN EJECTOR COOLING CYCLE DRIVEN BY HIGH-TEMPERATURE PARABOLIC TROUGH COLLECTORS WITH THERMAL ENERGY STORAGE

Konstantinos Braimakis[1,*], Dimitrios Tziritas[2], George M. Stavrakakis[2], Julio Terrón Gutiérrez[3], Siddharth Dutta[4], Christos Xynos[5], Panagiotis Zervas[2], Sotirios Karellas[5]

[1] *Laboratory of Refrigeration, Air Conditioning & Solar Energy*
National Technical University of Athens, Athens, Greece
[2] *MES ENERGY S.A., Athens, Greece*
[3] *CADE Soluciones de Ingeniería, S.L., Parque Científico y Tecnológico de Albacete, Albacete , Spain*
[4] *Protarget A.G., Cologne, Germany*
[5] *Laboratory of Thermal Processes*
National Technical University of Athens, Athens, Greece

*Corresponding Author: mpraim@central.ntua.gr

ABSTRACT

This study presents the development of the TES4Trig demonstrator that will be installed for covering the energy needs of the Administration building of the Lavrio Technological and Cultural Park (LTCP) in Attica, Greece within TES4Trig CSP-ERANET project. The system is driven by high-temperature parabolic trough collectors (PTC) coupled with innovative solid-state thermal energy storage (TES). Heat is supplied to an Organic Rankine Cycle (ORC) – Ejector cooling cycle (ECC) through a heat transfer fluid (HTF). The ORC-ECC is capable of the following operating modes: 1) electricity-only, 2) combined heat and power (CHP) and 3) cooling. The system energy production and consumer demand were considered for the conceptual design and preliminary definition of the operating strategies of the ORC-ECC. The final design of the ORC-ECC system is based on the use of R1233zd(E) as a working fluid, operating at a maximum temperature of 140°C.

1 INTRODUCTION

As of 2023, the vast majority of existing commercial concentrating solar power (CSP) plants (97 out of 105) are based on Steam Rankine Cycle (SRC) and are oriented toward large power capacities above 10 MW_e (IRENA, 2022). Despite the significant development of the technology in the last decades, the economics of CSP is still unfavorable, as it is associated with the highest levelized cost of electricity (LCOE) among other renewable power generation technologies, mainly due to its high capital investment cost (CAPEX).

Two main strategies to increase the cost-effectiveness of CSP plants include the increase of their thermal energy storage (TES) capabilities to improve their capacity factor as well as polygeneration, to produce heating and/or cooling in addition to electrical energy and thus increase their revenue. The latter option is usually infeasible in the case of large CSP plants that are typically located in remote locations (for example in desert areas) far from heating and cooling consumers because of their significant land requirement linked with their low energy density (77 kWh_e/m^2/year) (Lovering et al., 2022). Meanwhile, cost-effective, long-term TES technologies are needed to make CSP plants competitive against utility PV which typically include electrical batteries of limited storage capacity. Considering the above, polygeneration CSP plants at smaller scales that could service building energy consumers combined

with cost-effective TES could have significant market potential and improve the share of CSP in the energy mix.
At smaller scales, the Organic Rankine Cycle (ORC) is more suitable for thermal power generation than SRC, making it attractive for small-scale CSP plants. One of the most typically considered solar collector technology for such plants is parabolic trough collectors (PTCs), which offer good efficiencies at high heat transfer fluid (HTF) temperatures, up to 400°C (Kalogirou, 2023)(Kalogirou, Karellas, Badescu, et al., 2016; Kalogirou, Karellas, Braimakis, et al., 2016). Furthermore, in the last years, the cost of PTCs is declining, presenting opportunities for increasing the cost-competitiveness of the technology (Kurup & Turchi, 2015).
PTC-driven ORC plants for exclusive electricity production or polygeneration based on parabolic trough collectors (PTCs) have been extensively investigated at a theoretical level from a thermodynamic and techno-economic perspective. However, very few examples of experimental prototypes and real-world plants are available, especially considering polygeneration (Kasaeian et al., 2022) Aiming to fill this gap, this study presents the conceptual design and definition of the main operating strategies and main technical specifications of the TES4Trig demonstrator plant (TES4Trig Project, 2023), which will consist of a small-scale, PTC-driven ORC coupled with an ejector cooling cycle (ECC) into a singular ORC-ECC system for the production of electricity, heating and cooling. The demonstrator will also feature an innovative solid-state TES. The demo will service the energy needs of the Administration "Serpieri" Building of Lavrio Technological and Cultural Park (LTCP) in Attica, Greece in the context of a project funded by CSP ERANET (CSP ERANET, 2023).

2 TES4TRIG CONCEPTUAL DESIGN

2.1 Description of the demo site

The TES4Trig demo will be installed to cover the energy needs of the Administration (Admin) "Serpieri" building of the LTCP. The building houses several offices, seminar rooms and library/archive rooms. The area considered for installing the prototype is located at the west of the Admin building, which is sufficiently large for the installation of the solar field of the system. The Admin building was built in 1875 and has high symbolic and architectural value. As a result, great care had to be taken to ensure the harmonious integration of the TES4Trig system with them. 690

2.2 Heating, cooling and electrical energy demands

At present, the building's heating and cooling system consists of a heating oil boiler and a chiller and a hydronic distribution system to deliver hot/chilled water to the building terminal units (fan coil units-FCUs). The boiler has an average capacity of 93.04 kW_{th} and a maximum capacity of 125 kW_{th}. The chiller is a type HRA 0252 model from Climaveneta with a nominal cooling capacity of 61.6 kW_c.
For the needs of the project, the hourly variation of the heating and cooling demand of the building was calculated for 12 characteristic days of the year, each corresponding to a different month. Note that the electricity loads were not a critical factor in the design of the TES4Trig system because its scale is significantly lower than the electricity loads of the building. For the calculation of the heating load, DIN 4701 standard was implemented (DIN, 1995a, 1995b). For the calculation of the cooling load, CLTD/CLF method was implemented (ASHRAE, 1985). The hourly variation of the heating and cooling load of the building for the characteristic day of each month of the heating and cooling periods is illustrated in the diagrams of **Figure 1**.
The maximum heating demand occurs in January at 9:00 am and is about 70 kW_{th}. Generally, the maximum heating demand appears early in the morning, when the building occupants arrive and gradually declines until noon, owing to the solar radiation heat gains. Right after noon, as many of the building areas are not used, the demand abruptly declines, remaining approximately constant until 16:00, at which all users of the building leave.
As far as cooling demand is concerned, its maximum value is around 73 kW_c and occurs near noon in the summer months (July and August). Like the heating demand, the cooling demand abruptly declines after noon. According to calculations, the total annual heating, cooling and electricity demand are equal to 17580 kWh/year, 22720 kWh/year and 11540 kWh/year, respectively.

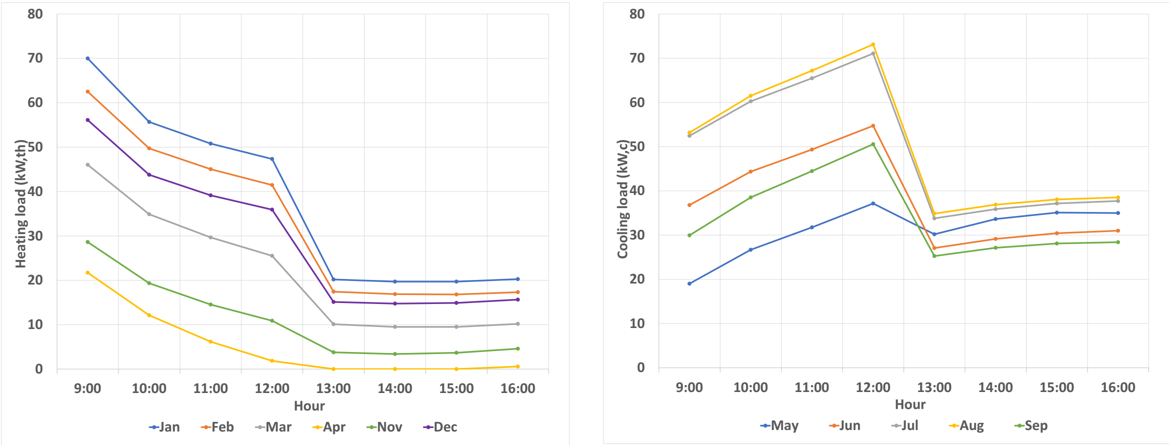

Figure 1: Heating (left) and cooling (right) loads for the characteristic day of each month

2.3 Parabolic trough collectors field

The solar field size was predetermined at the start of the project. It consists of two arrays of a total of 8 modules (4 modules/array) of single-axis tracking PTCs, each having an aperture of about 150 m^2 (total aperture of solar field is about 300 m^2. The PTCs are installed in an approximately N-S orientation, which is preferable for maximizing the annual solar thermal power production based on the available plot of land. The gross land surface occupied by the solar field (considering also necessary spacing of PTC arrays) is about 600 m^2. The peak and average solar thermal power output, as well as the generated energy by the solar field for the two corresponding to maximum (summer) and minimum (winter) solar irradiance throughout the year, are summarized in **Table 1**. The PTC field is capable of a maximum operating HTF temperature of about 400 °C. The project partner responsible for the development and manufacturing and installation of the solar field is the German industrial company Protarget AG (Protarget AG, 2023). 691

Table 1: Solar field main specifications

	Peak power (kW)	**Average power 08:00 – 18:00 (kW$_{th}$)**	**Generated energy (kWh$_{th}$)**
Summer	125	100	1000
Winter	90	51	510

2.4 Thermal energy storage

The TES, developed by project partner CADE Engineered Technologies (CADE Engineered Technologies, 2023) works in parallel with the PTC field and the ORC-ECC (**Figure 2**). Normally, when the solar power produced by the solar field is greater than the thermal demand of the ORC-ECC, the surplus solar power is stored in the TES. On the other hand, when the ORC-ECC thermal demand is higher than the solar power produced by the solar field, thermal energy is supplied from the TES to the ORC-ECC.

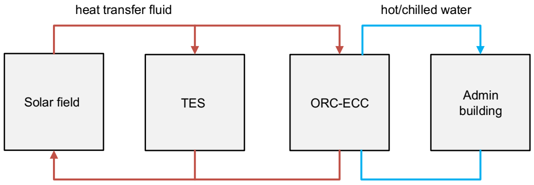

Figure 2: Simplified TES4Trig block diagram

2.5 ORC-ECC

The ORC-ECC system consists of an ORC coupled with an ECC. A recuperative ORC is implemented. The ECC is a thermally-driven cooling cycle, which is applied for the production of cooling through the exploitation of thermal energy and has been widely considered as a solar cooling technology (Braimakis, 2021). It is similar to the conventional vapor compression cycle; however, the mechanical compression of the latter is replaced by a dynamic compression occurring in an ejector device. In the TES4Trig project, an innovative ORC-ECC configuration is designed, which consists of an ORC coupled with an ECC. Both cycles run with the same working fluid and use a common heat exchanger as an ORC evaporator/ECC generator, as well as a common condenser, subcooler and pump.

The ORC-ECC has three operating modes: 1) electricity-only, 2) combined heat and power (CHP), and 3) cooling-only. In the first two modes, only the ORC is operational, while in the third mode, only the ECC is operational. In electricity-only mode, the ORC working fluid is heated in the ORC evaporator, passes through the expander, the recuperator hot-side and subsequently through the condenser and subcooler, exiting it as subcooled liquid which is then discharged by the ORC pump to the recuperator's cold-side. The CHP mode is similar, however, in this mode, the recuperator is bypassed and the condenser pressure/temperature is raised to produce heat at higher temperature. In cooling mode, the working fluid exiting the ORC evaporator is driven to the high-pressure inlet port of the ejector where it is mixed with low-temperature and pressure vapor coming from the ECC (cooling) evaporator that enters the low-pressure port of the ejector. In the ejector, the two streams are mixed and the resulting mixed vapor stream leaves the ejector at an intermediate pressure from its outlet port and is supplied to the condenser and subcooler. The subcooled liquid stream is pressurized in the pump and split into two streams. The first is conveyed to the ORC evaporator and the second to the ECC cooling evaporator.

A simplified schematic of the ORC-ECC configuration for the three different operating modes is shown in **Figure 3**. In each layout, the active sections of the system in each mode are highlighted. Note that the schematics shown in this figure are conceptual and do not represent the actual system. For each mode, the processes occurring are illustrated in temperature-entropy diagrams shown in the same figure.

2.6 -Integration of ORC-ECC with consumer building 692

The ORC-ECC system will be integrated into the existing heating and cooling building infrastructure through an intermediate water-glycol circuit, which is used for the interconnection between the refrigerant circuit (ORC-ECC) and the hydronic distribution network of the building. The water-glycol circuit includes a heating heat exchanger (for the provision of heating), a cooling heat exchanger (for the provision of cooling) and a dry cooler, which is used for rejecting excess heat to the ambient, as shown in **Figure 4**.

As it will be shown next, the cooling produced by the ECC is much smaller than the cooling demand of the building. Therefore, all cooling produced by the ECC is fully utilized. On the other hand, the heating produced by the ORC in CHP mode is comparable to the heating demand of the building. Consequently, because the heating demand of the building fluctuates, the flow rate of the water-glycol being supplied to the heating heat exchanger is adjusted through a three-way valve, while the remaining water-glycol flow is rejected through the dry cooler. At all times, the oil boiler and chiller of the building operate as auxiliary systems.

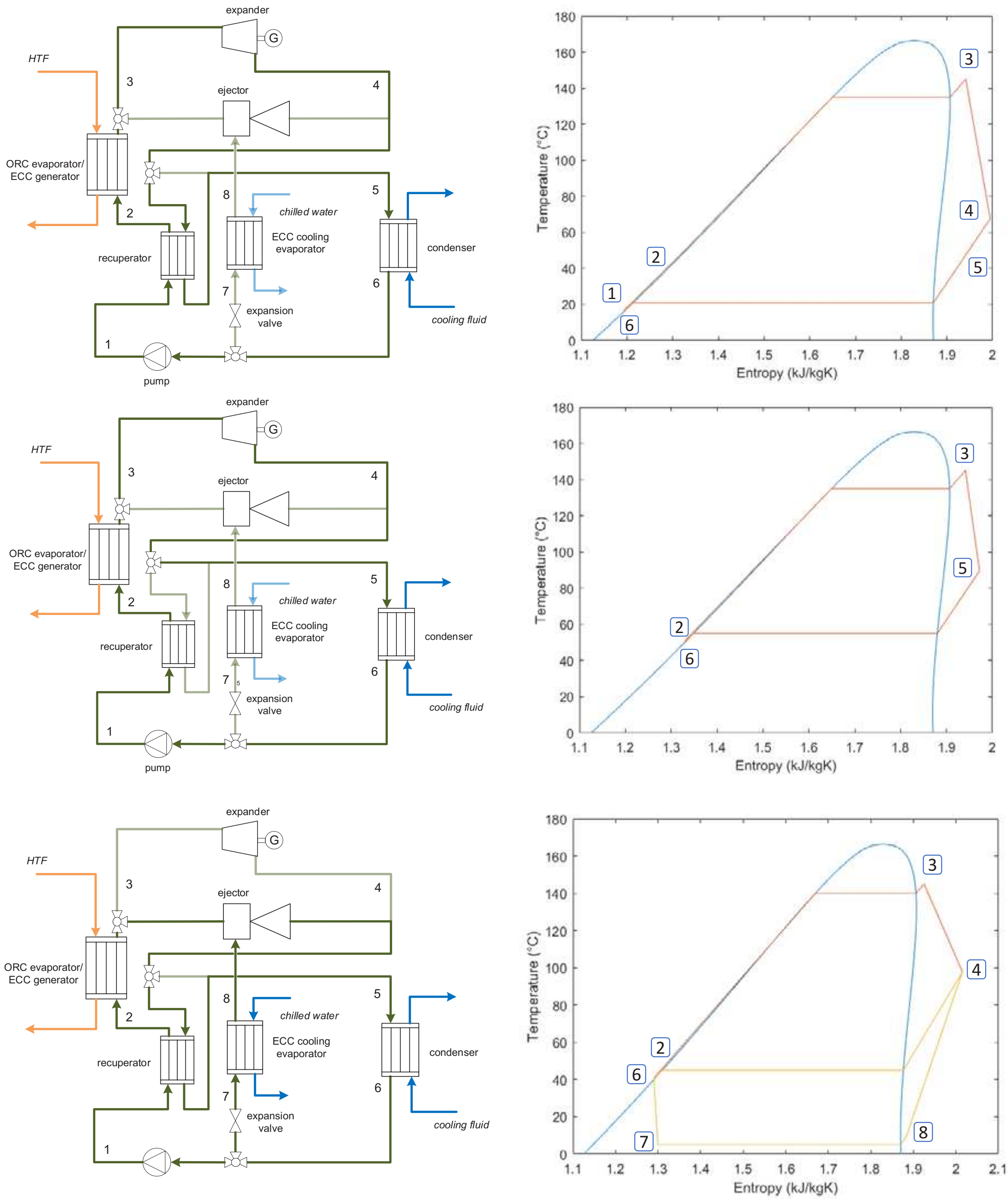

Figure 3: ORC-ECC layout and thermodynamic processes occurring in electricity-only mode (top), CHP mode (middle) and cooling mode (bottom)

3 TECHNICAL SPECIFICATIONS AND OPERATING STRATEGIES

3.1 Main technical specifications of ORC-ECC system

For the ORC-ECC, it was decided to use hydrofluoroolefin R1233zd(E) as a working fluid (Honeywell, 2018), as it is non-toxic, non-flammable and environmentally friendly (Braimakis et al., 2017). One of its drawbacks is its relatively lower efficiency for use in ORCs and ECCs because it has a lower critical temperature (167°C) and the fact that its maximum operating temperature is relatively limited to below

150-180°C because of its thermostability (Kim et al., 2018). Notably, the use of the particular low-critical temperature fluid instead of a working fluid of higher critical temperature (such as a hydrocarbon or siloxane) that would result in higher cycle efficiencies in the particular application which is driven by high-temperature PTCs is sub-optimal (Braimakis et al., 2017). Nevertheless, the safety of operation was prioritized over efficiency in the demonstrator because of its special characteristics (non-industrial environment, within a historical site and next to a building that is used as an office by non-trained personnel). Because of the aforementioned limitations, the maximum ORC-ECC cycle temperature was limited to 140°C. The detailed design specifications of the ORC-ECC for the three main operating modes are summarized in **Table 2**. The design specifications were determined by modeling the system in Matlab (*MATLAB - MathWorks*, 2023), using REFPROP (Huber et al., 2022) for the calculation of all thermophysical properties and the 1-D ejector model by Huang et al. (Huang et al., 1999).
Briefly, in the electricity-only and CHP modes, the cycle's maximum temperature is 135 °C and a superheating degree of 10 K is applied, while the condensation temperature is 21/40°C (winter/summer) and 55°C, respectively. Regarding the ECC, the maximum cycle temperature is slightly increased to 140°C and a lower superheating degree is applied (5 K), while a condensation temperature of 45°C is assumed.

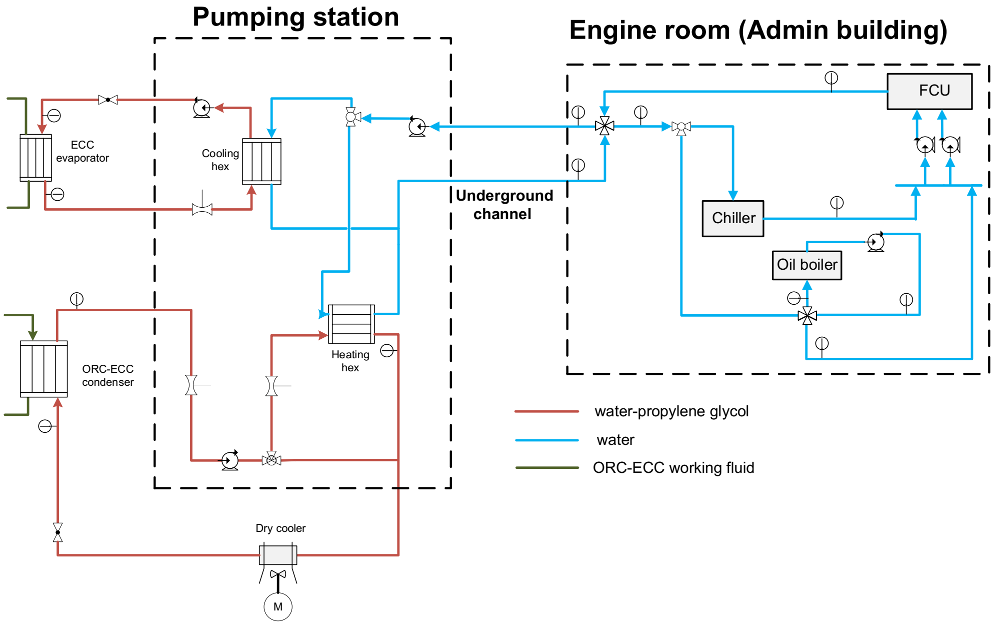

Figure 4: Simple schematic of the integration layout of the ORC-ECC with the building

Critical limitations regarding the ORC upper and lower pressure selection arise because of expander limitations at the targeted power range (about 5-20 kW). In the project, two similar twin-screw expanders with different built-in volume ratios will be used, which are modified commercial compressor models produced by Bitzer. The first is an OSK-5361 model (built-in volume ratio=3.5) that had been used in a past experimental test rig by TUM (Dawo et al., 2021) and the second is an OSN-5361 model (built-in volume ratio 5.6) offered to NTUA by Bitzer (Bitzer, 2023)(TAIRIS AEBE, 2023).
In the following equations, the basic performance indexes are presented based on which the efficiency of the whole system is calculated.
The heat supplied to the ORC-ECC :

$$\dot{Q}_{in} = \dot{m}_{HTF} \cdot \left(h_{HTF}^{in} - h_{HTF}^{out}\right) = \dot{m}_{WF} \cdot (h_2 - h_1) \quad (1)$$

The net electric power produced by the ORC is given by the following equation:

$$P_{e,net} = \dot{m}_{WF} \cdot \left[(h_3 - h_4) \cdot n_{em} - \frac{(h_1 - h_6)}{n_{pump}}\right] \quad (2)$$

The cooling output in the ECC evaporator is given by the following equation:

694

$$\dot{Q}_c = \dot{m}_{WF} \cdot (h_8 - h_7) \quad (3)$$

The useful heat produced by the condenser in CHP mode is given by the following equation:

$$\dot{Q}_h = \dot{m}_{WF} \cdot (h_5 - h_6) \quad (4)$$

The two main performance indexes of the system are the electric efficiency of the ORC and the thermal coefficient of performance (COP) of the ECC. These are defined according to the following equations:

$$\eta_e = \frac{P_{e,net}}{\dot{Q}_{in}} \quad (5)$$

$$COP_{th} = \frac{\dot{Q}_c}{\dot{Q}_{in}} \quad (6)$$

3.2 Sizing and operating strategies

The starting point for sizing the TES4Trig demonstrator and the definition of its operating strategies was the size of the solar field (determined a priori) and the heating/cooling demand of the building. For the needs of the project, two objectives were prioritized: 1) high annual solar energy utilization, and 2) covering substantial shares of the heating and cooling demand of the building, while also producing as much electrical energy as possible. The following operating strategy was thus defined for the preliminary sizing of the ORC-ECC system:

- Throughout the whole year, the ORC-ECC is operational whenever sufficient thermal power is available either from the solar field or from the TES.
- To ensure the reliability of operation, the ORC operates under a relatively constant thermal input (corresponding to the design thermal input point) with a cut-off threshold of 75% of the design. On the other hand, the ECC operates exclusively at the design point. Meanwhile, the operating mode of the ORC-ECC (and thus the produced useful energy) changes depending on the demand status of the building between electricity-only, CHP and cooling modes.
    - When there is neither heating nor cooling demand, the ORC-ECC produces electricity.
    - When there is heating demand, the ORC-ECC operates in CHP mode. If the produced heat is higher than the heating demand, the excess heat generated in the condenser is rejected to the ambient through the dry cooler. If the produced heat is lower than the heating demand, the ORC-ECC provides all the heat it can to the building and the remaining heat demand is covered by the oil boiler.
    - When there is cooling demand, the ORC-ECC operates in ECC mode. Since the cooling output of the ECC is much lower than the cooling demand, all produced cooling is utilized for covering the cooling demand of the building, while the remaining cooling demand is covered by the chiller of the building.

Table 2: ORC-ECC design specifications

<table>
<tr><th>Parameter</th><th>Electricity-only</th><th>CHP</th><th>Cooling-only</th></tr>
<tr><td>HTF inlet/outlet temperature (°C)</td><td colspan="3">400/350</td></tr>
<tr><td>Maximum working fluid temperature (°C)</td><td colspan="2">135</td><td>140</td></tr>
<tr><td>Maximum fluid pressure (bar)</td><td colspan="2">17.4</td><td>20.9</td></tr>
<tr><td>Working fluid superheating degree at ORC evaporator/ECC generator outlet (K)</td><td colspan="2">10</td><td>5</td></tr>
<tr><td>Expander model used</td><td>OSN-5361 (winter)
OSK-5361 (summer)</td><td>OSK-5361</td><td>-</td></tr>
<tr><td>Condensation temperature (°C)</td><td>21 (winter)
40 (summer)</td><td>55</td><td>45</td></tr>
<tr><td>Cold stream temperature rise in recuperator (K)</td><td>30 (winter)
20 (summer)</td><td>0</td><td>25</td></tr>
<tr><td>Cooling evaporator saturation temperature (°C)</td><td colspan="2">-</td><td>5</td></tr>
<tr><td>Cooling evaporator superheating degree (K)</td><td colspan="2">-</td><td>2</td></tr>
<tr><td>Subcooling degree at pump inlet (K)</td><td colspan="3">5</td></tr>
<tr><td>Expander isentropic efficiency (%)</td><td colspan="2">65</td><td>-</td></tr>
<tr><td>Generator electromechanical efficiency (%)</td><td colspan="2">96</td><td></td></tr>
<tr><td>Pump isentropic efficiency (%)</td><td colspan="3">65</td></tr>
<tr><td>Pump motor electromechanical efficiency</td><td colspan="3">85</td></tr>
<tr><td>Water-glycol temperature at ECC evaporator inlet/outlet (°C)</td><td colspan="2"></td><td>13/8</td></tr>
<tr><td>Hot/chilled water return/supply temperature to/from building hydraulic network (°C)</td><td>-</td><td>47/52(hot water)</td><td>18/17.4 (chilled water)</td></tr>
<tr><td></td><td></td><td></td><td></td></tr>
<tr><td>Water-glycol temperature at condenser inlet/outlet (°C)</td><td>13/18 (winter)
32/47 (winter)</td><td>47/52</td><td>37/42</td></tr>
<tr><td>ORC electric efficiency (%)</td><td>13.6 (winter)
10.7 (summer)</td><td>8.9</td><td>-</td></tr>
<tr><td>Heating efficiency (%)</td><td>-</td><td>87.4</td><td>-</td></tr>
<tr><td>ECC ejector entrainment ratio (-)</td><td colspan="2">-</td><td>0.13</td></tr>
<tr><td>ECC thermal COP (-)</td><td colspan="2">-</td><td>0.10</td></tr>
</table>

Regarding the thermal input to the ORC-ECC by the solar field and TES, the following operating strategy is applied:

- If there is no sun (no SF solar thermal power - $\dot{Q}_{SF} = 0$) the following cases are distinguished:
  - If the available thermal power from the TES ($\dot{Q}_{TES} = 0$) is lower than the minimum required by the ORC-ECC ($\dot{Q}_{min}$), the TES is idle while the ORC-ECC is not operational (**No operation mode**).
  - If the available thermal power from the TES is higher than the minimum required by the ORC-ECC ($\dot{Q}_{TES} > \dot{Q}_{min}$), the TES drives the ORC-ECC (**TES production and discharge mode**). The following cases are distinguished regarding the ORC-ECC:
    - If the available thermal power from the TES is lower than the nominal required by the ORC-ECC ($\dot{Q}_{nom} > \dot{Q}_{TES} > \dot{Q}_{min}$), the ORC-ECC operates in part-load (**TES production and discharge mode A**).

- If the available thermal power from the TES is higher than the nominal required by the ORC-ECC ($\dot{Q}_{TES} > \dot{Q}_{nom}$), the ORC-ECC operates in full load (**TES production and discharge mode B**).

- If there is sun ($\dot{Q}_{SF} > 0$) the following cases are distinguished:
  - If the SF solar thermal power is lower than the minimum required by the ORC-ECC ($\dot{Q}_{SF} < \dot{Q}_{min}$), the following cases are distinguished:
    - If the sum of the SF solar thermal power and available thermal power from the TES is lower than the minimum required by the ORC-ECC ($\dot{Q}_{SF} + \dot{Q}_{TES} < \dot{Q}_{min}$), the ORC-ECC is not operational and the TES is charged (**Charge mode**).
    - If the sum of the SF solar thermal power and the available thermal power from the TES is higher than the minimum required by the ORC-ECC but lower than the nominal ($\dot{Q}_{nom} > \dot{Q}_{SF} + \dot{Q}_{TES} > \dot{Q}_{min}$), the ORC-ECC operates in part-load and is driven by both the SF and TES (**SF-TES production and discharge mode**).
  - If the SF solar thermal power is higher than the minimum required by the ORC-ECC but lower than the nominal ($\dot{Q}_{nom} > \dot{Q}_{SF} > \dot{Q}_{min}$), the SF solar thermal power is used for driving the ORC-ECC, which operates in part-load. No heat is stored (**SF production mode**).
  - If the SF solar thermal power is higher than the nominal required by the ORC-ECC ($\dot{Q}_{SF} > \dot{Q}_{nom}$), the needed SF solar thermal power is used for driving the ORC-ECC while the surplus solar thermal power ($\dot{Q}_{SF} - \dot{Q}_{nom}$) is stored in the TES (**SF production and charge mode**).

In the flowchart of **Figure 5** the described operation strategy is illustrated.

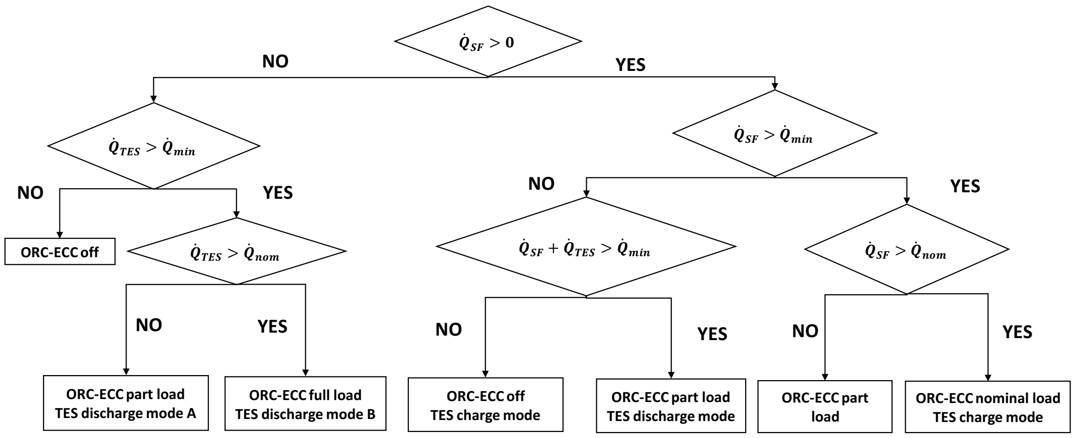

Figure 5: Flowchart of the operating strategy

3.3 TES4Trig demonstrator overall conceptual design and operating strategies

Based on the aforementioned considerations, the ORC-ECC was sized based on a nominal thermal input of 75 kW_{th}, equal to the nominal thermal power capacity of the TES, which will have a total energy storage capacity of 400 kWh_{th}. Based on the specifications shown in **Table 2**, the power, heating and cooling output of the system is presented in **Table 3**.

Table 3: Electric power, heating and cooling output of TES4Trig system (nominal)

Parameter	Electricity-only	CHP	Cooling-only
Electric power output (kW_e)	10.2 (winter) 8.0 (summer)	6.7	-
Heating output (kW_{th})	-	65.6	-
Cooling output (kW_c)	-	-	7.7

697

3.4 Experimental validation and challenges

The commissioning of the prototype is planned for Q1 2024. Comissioning tests are necessary to fully define the control of each subsystem and the overall prototype. Following commissioning, the prototype will be demonstrated for the following years to evaluate its performance under variable conditions of solar availability for different cases of the building energy demand for all operational modes.

To date, the most challenging aspect of the project is the integration of the prototype into the consumer building. Because of the architectural and historical value of the building, great care had to be taken to minimize aesthetic disruption of the location. This necessitated the development of a very long underground channel to house piping and cables (power supply, automation) since it was not acceptable to carry out any non-reversible interventions on the building itself. Secondly, integration challenges arise because of the sophisticated automation, large number of equipment components (valves, sensors) and complexity of the piping interconnection layout with the existing infrastructure of the building, considering all different operating modes and the need for providing heating and cooling at specific temperatures. An additional challenge is the development of fully automated control, which should orchestrate all different subsystems of the prototype (solar field, thermal energy storage, ORC-ECC) as well as the consumer building itself.

Regarding the ORC-ECC, the major challenge was the difficulty of developing a micro-scale ORC to be driven by a very high-temperature heat source, which was the original scope of the project. This is because of several reasons. First, there is currently very limited (if any) availability of micro-scale expansion machines capable of operating at very high temperatures above 140°C. Secondly, because of the installation of the prototype in a non-industrial site, safety precautions dictated the use of non-flammable working fluids, excluding the use of alkanes which are suitable for high temperatures. As a result, the system was eventually designed for operation at a maximum temperature of 140°C. This decision required the use of a sophisticated, tailor-made evaporator, because of the significantly high-temperature difference between the working fluid and the HTF.

4 CONCLUSIONS

698

In the present work, the conceptual design, operating strategy and sizing of the TES4Trig prototype and its subsystems were described. The system will be installed for covering the energy needs of the Admin building of the Lavrio Technological and Cultural Park (LTCP).

NOMENCLATURE

Abbreviations

CHP	Combined Heat & Power
ECC	Ejector Cooling Cycle
HTF	Heat Tranfer Fluid
LTCP	Lavrio Technological and Cultural Park
ORC	Organic Rankine Cycle
PTC	Paracolic Trough Collectors
SF	Solar Field
TES	Thermal Energy Storage

Variables

COP	Coefficient of performance	(-)
h	specific enthalpy	(kJ/kg)
$\dot{m}$	mass flow rate	(kg/s)
P	power	(kW)
$\dot{Q}$	heat duty	(kW)

Greek letters

η	efficiency	(-)

Subscript

c	cooling
e	electric
em	electromechanical (expander-generator)
h	heating
HTF	heat transfer fluid
in	input, inlet
min	minimum thermal power required for driving the ORC-ECC
n	net
net	net
nom	nominal thermal power required for driving the ORC-ECC
out	outlet
pump	pump
SF	thermal power produced by solar field
TES	thermal power available from thermal energy storage
th	thermal
WF	working fluid

REFERENCES

ASHRAE. (1985). *American Society of Heating, Refrigerating and Air-Conditioning Engineers, 1985 ASHRAE Handbook: Fundamentals, Atlanta: American Society of Heating, Refrigerating and Air-Conditioning Engineers, 1985.*

Bitzer. (2023). *BITZER*. https://www.bitzer.de/gb/en/

Braimakis, K. (2021). Solar ejector cooling systems: A review. *Renewable Energy*, *164*, 566–602. https://doi.org/10.1016/j.renene.2020.09.079

Braimakis, K., C. Roumpedakis, T., Leontaritis, A.-D., & Karellas, S. (2017). Comparison of Environmentally Friendly Working Fluids for Organic Rankine Cycles. *Advances in New Heat Transfer Fluids*, 377–426. https://doi.org/10.1201/9781315368184-13 699

CADE Engineered Technologies. (2023). *https://cadeengineering.com/.*

CSP ERANET. (2023). *https://csp-eranet.eu/results/thermal-energy-storage-demand-solar-trigeneration-tes4trig.*

Dawo, F., Eyerer, S., Pili, R., Wieland, C., & Spliethoff, H. (2021). Experimental investigation, model validation and application of twin-screw expanders with different built-in volume ratios. *Applied Energy*, *282*, 116139. https://doi.org/10.1016/J.APENERGY.2020.116139

DIN. (1995a). *DIN 4701-1 Rules for calculating the heat load of buildings- Part 1: Basic rules for calculation*.

DIN. (1995b). *DIN 4701-2 Rules for calculating the heat requirement of buildings - Part 2: Tables, pictures, algorithms*.

Honeywell. (2018). *A Better Environment with Next-Generation Solstice® zd Refrigerant Solstice zd: Compliant with Regulations*.

Huang, B. J., Chang, J. M., Wang, C. P., & Petrenko, V. A. (1999). A 1-D analysis of ejector performance. *International Journal of Refrigeration*, *22*(5), 354–364. https://doi.org/10.1016/S0140-7007(99)00004-3

Huber, M. L., Lemmon, E. W., Bell, I. H., & McLinden, M. O. (2022). The NIST REFPROP Database for Highly Accurate Properties of Industrially Important Fluids. *Industrial and Engineering Chemistry Research*, *61*(42), 15449–15472. https://doi.org/10.1021/ACS.IECR.2C01427

IRENA. (2022). *Renewable Power Generation Costs in 2021*.

Kalogirou, S. A. (2023). *SOLAR ENERGY ENGINEERING : processes and systems.*

Kalogirou, S. A., Karellas, S., Badescu, V., & Braimakis, K. (2016). Exergy analysis on solar thermal systems: A better understanding of their sustainability. *Renewable Energy*, *85*, 1328–1333. https://doi.org/10.1016/J.RENENE.2015.05.037

Kalogirou, S. A., Karellas, S., Braimakis, K., Stanciu, C., & Badescu, V. (2016). Exergy analysis of solar thermal collectors and processes. *Progress in Energy and Combustion Science*, *56*, 106–137. https://doi.org/10.1016/J.PECS.2016.05.002

Kasaeian, A., Mirjavadi, K., Pourmoghadam, P., Asgari Sima, F., Amirhaeri, Y., Borhani, S., & Fereidooni, L. (2022). Organic Rankine cycles powered by parabolic trough collectors: An overview. *Sustainable Energy Technologies and Assessments*, *54*, 102847. https://doi.org/10.1016/J.SETA.2022.102847

Kim, S., Rached, W., & Abbas, L. (2018). Performance and Stability of E-1233zd in Energy Recovery Applications. *International Refrigeration and Air Conditioning Conference*. https://docs.lib.purdue.edu/iracc/2053

Kurup, P., & Turchi, C. S. (2015). *Parabolic Trough Collector Cost Update for the System Advisor Model (SAM)*. https://doi.org/10.2172/1227713

Lovering, J., Swain, M., Blomqvist, L., & Hernandez, R. R. (2022). Land-use intensity of electricity production and tomorrow's energy landscape. *PLOS ONE*, *17*(7), e0270155. https://doi.org/10.1371/JOURNAL.PONE.0270155

MATLAB - MathWorks. (2023). https://www.mathworks.com/products/matlab.html

Protarget AG. (2023). *https://protarget-ag.com/*.

TAIRIS AEBE. (2023). *Ταΐρης ΑΕΒΕ – Κορυφαίες λύσεις ψύξης, κλιματισμού & θέρμανσης σε όλους τους κλάδους την βιομηχανίας*. https://www.tairis.gr/en/enhome/

TES4Trig Project. (2023). *Thermal Energy Storage for On-demand Solar Trigeneration (TES4Trig), http://www.solar.demokritos.gr/ERANET/*.

ACKNOWLEDGEMENT

The study has been funded by the TES4Trig project within the CSP ERANET 1st Joint Call.

This book contains the compilation of works contributed to the *7th International Seminar on Organic Rankine Cycle Power Systems* (ORC 2023), held in Seville between the 4th and 6th of September 2023. The event was hosted by Universidad de Sevilla on behalf of the Knowledge Centre on Organic Rankine Cycle Technology (KCORC), incorporated in The Netherlands.

The ORC conference, organized biennially, stems as the only conference that is specific to ORC technology, therefore gathering a diverse community whose affiliation spans across all the interested stakeholders, not only in this particular technology but also and in a broader context, in the energy transition. Original equipment manufacturers, professional associations, end-users, investors, policy makers, academics, scientists feel at home at ORC 2023.

The almost 100 proceedings in this book cover a wide variety of topics, from fundamentals to system integration through component design, accounting for thermodynamic performance as well as component design. In addition to this, and as a new track in 2023, works on heat pump technology were also accepted in order to raise awareness of the strong ties between both technologies, specifically in energy storage applications.

This book provides an excellent overview of the current maturity of power systems based on Organic Rankine Cycle technology for applications as diverse as geothermal and waste heat recovery in industry or downstream of other prime movers (e.g., marine applications). It is also an excellent source of information to understand the current challenges faced by the technology, stemming from a very competitive market and increasingly stringent environmental regulations.

The organizers of ORC 2023 hope that the reader finds this work as exciting as the attendees to the conference and, maybe, make the decision to join the 8th edition to the conference in 2025.

KCORC
KNOWLEDGE CENTER
ORGANIC RANKINE CYCLE

eUS EDITORIAL
UNIVERSIDAD DE SEVILLA